

03-170

# Environment Canada

Water Science and  
Technology Directorate

---

Direction générale des sciences  
et de la technologie, eau

## Environnement Canada

TD  
226  
N87  
no.  
03-170

The Geochemistry of Acid Mine Drainage

By:

D. Blowes, C. Ptacek, J. Jambor, C. Weisener

NWRI Contribution # 03-170

03-170

## Géochimie du drainage minier acide

D.W. Blowes, C.J. Ptacek, J.L. Jambor et C.G. Weisener

# Sommaire des recherches de l'INRE

### Titre en langage clair

Géochimie du drainage minier acide

#### Quel est le problème et que savent les chercheurs à ce sujet?

Des acides et des métaux toxiques continuent à être rejetés par d'anciens sites miniers pendant des décennies et même des siècles après la fin de l'exploitation minière. Il existe un nombre énorme de sites miniers dans le monde. Par exemple, il y a au Canada plus de 10 000 sites miniers, attestés par des documents, et aux États-Unis plus de 500 000. La production de drainage minier acide varie d'un site à l'autre et est fonction d'une combinaison de divers processus physiques, géochimiques et microbiologiques. Il existe de nombreuses données sur les processus conduisant à la production du drainage minier acide et au rejet de métaux toxiques dans les écosystèmes aquatiques.

#### Pourquoi l'INRE a-t-il effectué cette étude?

Les présentes recherches ont été entreprises pour réunir de l'information sur les nombreux aspects de ce drainage, sous la forme d'une étude complète. Les sujets examinés dans l'étude comprennent : les descriptions des caractéristiques d'un site minier, à savoir s'il s'agit d'une mine à ciel ouvert, d'une mine souterraine, d'amas de stériles, de résidus miniers ou de déchets de raffinage; la description des processus physiques, géochimiques et microbiologiques conduisant à l'oxydation des minéraux à base de sulfures, à la production d'acides, à la neutralisation des acides, à l'atténuation des métaux ainsi qu'à leur rejet et à leur absorption dans les écosystèmes aquatiques. Le présent document possède l'originalité de réunir les données produites dans de nombreux domaines scientifiques en un ensemble complet permettant de faciliter la communication de l'information à une large audience.

#### Quels sont les résultats?

La majorité des études sur le drainage minier acide ont été axées sur les acides produits par oxydation des pyrites et d'autres minéraux de type sulfure, sur la neutralisation des acides et enfin sur les mécanismes d'absorption des métaux. Les études ont été effectuées principalement sur des systèmes artificiels en laboratoire ou dans des lacs et cours d'eau contaminés. On dispose de moins de données sur les processus qui interviennent dans les ouvrages souterrains et dans les amas de déchets.

#### Comment ces résultats seront-ils utilisés?

L'information peut être utilisée pour identifier de futurs domaines de recherche, ou comme manuel par les spécialistes dans le secteur de la géochimie environnementale afin d'améliorer la gestion des sites miniers.

#### Quels étaient nos principaux partenaires dans cette étude?

Université de Waterloo, Université de Colombie-Britannique.

## 5. The Geochemistry of Acid Mine Drainage

D. W. Blowes

University of Waterloo, Waterloo, ON, Canada

C. J. Ptacek

University of Waterloo, Waterloo, ON, Canada

J. L. Jambor

University of British Columbia, Vancouver, BC, Canada

C. G. Weisener

University of Waterloo, Waterloo, ON, Canada

### 5.1 INTRODUCTION

#### 5.1.1 *Scale of the Problem*

Mine wastes are the largest volume of materials handled in the world (ICOLD, 1996). The generation of acidic drainage and the release of water containing high concentrations of dissolved metals from these wastes is an environmental problem of international scale. Acidic drainage is caused by the oxidation of sulfide minerals exposed to atmospheric oxygen. Although acid drainage is commonly associated with the extraction and processing of sulfide-bearing metalliferous ore deposits and sulfide-rich coal, acidic drainage can occur wherever sulfide minerals are excavated and exposed to atmospheric oxygen. Engineering projects, including road construction, airport development and foundation excavation, are examples of civil projects that have resulted in the generation of acidic drainage. On United States Forest Service Lands there are between 20,000 and 50,000 mines releasing acidic drainage (USDA, 1993). Kleinmann (1991) estimated that more than 6,400 km of rivers and streams in the eastern United States have been adversely affected by mine drainage water. Between 8,000 and 16,000 km of streams have been affected by metal mining in the western United States. The annual worldwide production of

mine wastes exceeded 4.5 billion tonnes in 1982 (ICOLD, 1996). Estimated costs for remediating mine wastes internationally total in the tens of billions of dollars (Feasby, 1993).

### *5.1.2 Overview of the Mining Process and Sources of Low-Quality Drainage*

The recovery of metals from sulfide-rich ore bodies proceeds through a series of steps: from mining to crushing to mineral recovery, followed typically by smelting of the sulfide ores, and thence to metal refining; although the nature of the ore body dictates the processes used to extract metals from ore, each of these steps generates a waste stream. The volumes of the waste streams can be large. For example, production of one tonne of copper typically requires the excavation and processing of 100 tonnes of rock. Each of the steps of metal production can lead to the generation of low-quality water.

#### *5.1.2.1 Mine workings and open pits*

Minerals are typically excavated by underground mining, strip mining, or open-pit mining. The selection of the mine design is dictated by the physical structure and value of the ore body and by the characteristics of the adjacent geological materials. Although open-pit mines and underground mines are the two most common mining strategies, placer mining and solution mining also have been used for mineral extraction. Placer mining involves excavation of river or stream sediments and the separation of valuable minerals by gravity, selective flotation, or by chemical extraction. Most solution mining is by heap leaching, in which the extractant solution is trickled over broken ore on the surface or in underground workings; less common is injection into underground aquifers. The consequence of the excavation of open pits and other mining-

related disturbances is that sulfide minerals previously isolated from the atmosphere are exposed to oxygen. Oxidation of sulfide minerals ensues.

#### *5.1.2.2 Waste rock*

Open-pit and underground mining result in the excavation of large volumes of rock to gain access to ore bodies. After the ore body is accessed, ore for processing is separated from the host rock on the basis of economic cut-off values. Rock of higher metal grade is processed, and rock below the cut-off grade is put to waste. Frequently, ore is segregated into high-grade and low-grade ore stockpiles. Ore is material that will yield a profit; thus, the metal contents of the discrimination between high-grade and low-grade ores will vary with the costs of mining activities and the value of the metals extracted. The waste rock from mine operations may be used in construction activities at the minesite. Excess waste rock is deposited in waste-rock piles whose composition differs greatly from mine to mine because of variations in ore-deposit and host-rock mineralogy, and because of differences in the processing techniques and ore-grade cut-off values. Daily production of waste rock in Canada is estimated to be 1,000,000 tonnes (Government of Canada, 1991). Because of the large volume of rock excavated in open-pit operations, waste-rock piles may be tens of hectares in area and tens of meters in height (Ritchie, 1994). For example, the Bingham Canyon open pit that is mined by Kennecott Utah Copper is 3100 m in diameter and 850 m deep. Approximately 5.2 billion tonnes of rock have been excavated from the pit, and 1.7 billion tonnes of this mass have been processed as ore. The remaining 3.5 billion tonnes are contained in waste-rock piles at the minesite. These piles cover an area of 2500 ha and are up to 300 m in height (M. Logsdon, pers. comm.).

### *5.1.2.3 Mill tailings*

The ore extracted in most non-ferrous, metalliferous mining operations is rich in base or precious metals, but the ore minerals are generally too dilute for direct processing using metallurgical techniques. Thus, most ores are processed through concentration steps that involve costs crushing, grinding, and milling to a fine grain size for beneficiation. The grain size of the milled rock is dictated by the process used for mineral recovery. Typical grain sizes range from 25  $\mu\text{m}$  to 1.0 mm. At many plants, differential flotation is used to separate the valuable sulfide minerals containing base or precious metals from others (e.g., pyrite  $[\text{FeS}_2]$  or pyrrhotite  $[\text{Fe}_{1-x}\text{S}]$ ) that have little commercial value. A flotation concentrator may contain several circuits for the selective recovery of a variety of metal sulfides and the production of a series of metal-sulfide concentrates. The concentrate from the flotation step is retained for further metallurgical processing. Mill tailings are the residual material, including sulfide gangue minerals, that is discharged to tailings impoundments, typically as a slurry of water and finely ground rock.

The ratio of tailings to concentrate can be very large, particularly at gold and precious-metal mines, at which the concentrate may represent only on small fraction of 1% of the ore processed. The mining industry produces immense masses of mine tailings. The mass of tailings produced daily in Canada is estimated to be 950,000 tonnes (Government of Canada, 1991). Tailings impoundments may be very large. For example, the Inco Ltd. Central Tailings Disposal Area covers an area of 25  $\text{km}^2$  with tailings up to 50 m in depth, and the ultimate capacity is more than 725 million tonnes (Puro et al., 1995).

Mill tailings are typically retained in impoundments. The retaining dams of many impoundments are constructed of coarse-grained tailings or of tailings combined with waste rock. These types of impoundments are designed to drain, thereby enhancing their structural integrity,

but resulting in the development of a thick zone of only partial saturation. The entry of gas-phase oxygen into the unsaturated tailings results in sulfide-mineral oxidation and the release of low-quality drainage.

## 5.2. MINERALOGY OF ORE DEPOSITS

### 5.2.1 Coal

Coal is an organic rock-like natural product (Speight, 1994) whose beginnings were as the remains of flora that accumulated as peat. The accumulation occurred in submerged conditions, thereby preventing complete decay of the organic material to  $\text{CO}_2 + \text{H}_2\text{O}$  during the early stage of maturation. Reflecting its origin, coal occurs in beds; maximum thicknesses approximate 90 m, and typical mining thicknesses are 1 to 4 m.

The carbon content of coal varies from about 70% to 95 wt%, with most of the remainder consisting of O, H, N, and S. The O content generally ranges from about 2 to 20%, and the major change that occurs during coalification is a decrease in the O content and an increase in the carbon content. With this change the physical properties and thermal yield per unit weight also change, and various classifications have been devised to reflect those properties. A common commercial subdivision is into 'brown coal' and 'hard coal', which in turn is an indication of the degree of induration. At the lowest end is brown coal, which has the lowest C and the highest moisture contents, and is most commonly classified as lignite. The upward progression is to sub-bituminous, bituminous, and anthracite, with the last the most highly evolved and of highest metamorphic rank. Most brown coal is lignite, with some overlap into the sub-bituminous category, whereas the others are hard coal. Most mined coal is of the bituminous variety.

Current world production is about 3500 Mt (million metric tonnes) of hard coal and about

900 Mt of brown coal. Germany, at about 160 Mt, is the largest producer of brown coal, with Russia a distant second. China's production of 900–1000 Mt of hard coal is the world's highest, with >90% obtained from underground mines. US production is a close second to that of China, whereas India ranks third and produces <300 Mt. In recent years the US has undergone a pronounced shift to mining of western coal, predominantly sub-bituminous, which has a lower average content of sulfur than coals from Appalachia. Wyoming alone now accounts for about a third of all US production.

Environmental concerns have been focused on the gaseous and particulate emissions, on the environmental quality of the ash and slag residues, and on acid drainage that may ensue as a consequence of the exposure of mining-related wastes to atmospheric weathering. Many of the environmentally least desirable aspects concerning the utilization of coal are related to the presence of mineral matter, especially Fe disulfides. The disulfides are a principal source for SO<sub>2</sub> emissions during combustion, and in mine wastes the oxidation of FeS<sub>2</sub> is the principal cause of the development of acidic drainage.

Stach et al. (1982) list more than 40 minerals that have been identified as occurring in coal, and recent observations have expanded the total to more than a hundred. Finkelman (1980a,b) concluded that coals yielding >5 wt% ash have had the bulk of their minerals derived by detrital processes.

Table 1 summarizes and presents an interpretation of the occurrence of the principal non-detrital minerals in coal. The chief detrital minerals are quartz and clay minerals (including K-Al micas), and these minerals commonly form up to 90% of the mineral matter in coals. The bulk of the remainder typically consists of carbonates and pyrite. Renton (1982) observed that most discrete mineral grains observed in coal are about 20 µm in diameter, and few exceed 100 µm.



Exceptions are concretions, nodules, and 'balls' that typically contain one or more of pyrite, marcasite [FeS<sub>2</sub>], calcite [CaCO<sub>3</sub>], and siderite [FeCO<sub>3</sub>], and which may be many centimeters in diameter. As well, aggregates of pyrite and marcasite occur within coal and as fracture (cleat) mineralization. The most common cleat-filling minerals are calcite, pyrite, and kaolinite [Al<sub>2</sub>Si<sub>2</sub>O<sub>5</sub>(OH)<sub>4</sub>] (Renton, 1982). Vassilev et al. (1996) observed that higher rank coals are enriched in elements associated with probable detrital minerals, whereas lower rank coals are enriched in elements associated with probable authigenic minerals and organic material.

Modern technology utilizes fluidized bed boilers, pressurized fluidized bed boilers, and gasification of coal to improve energy extraction and minimize potential pollutants. The lower temperatures of those processes affect the fate of the individual trace elements that are emitted or are associated with the residues from the consumed coal (Clarke, 1993).

### *5.2.2 Base-metal deposits*

Base metal is a wide-ranging term that refers either to metals inferior in value to those of gold and silver, or alternatively, to metals that are more chemically active than gold, silver, and the platinum metals (AGI, 1957). Accordingly, a review of base-metal mineralogy would encompass much of the world's metal production and geology. Usage of the 'base metal' term in the minerals industry is rather loose, but a common application is to the non-ferrous ore metals that include copper, lead, and zinc. Thus, for example, Kesler (1994) grouped manganese, nickel, chromium, silicon, cobalt, molybdenum, vanadium, tungsten, niobium, and tellurium as ferroalloy metals, and copper, lead, zinc, and tin as base metals. Among the latter four metals, tin is by far the least significant in terms of volumes consumed and monetary value.

World mine production of copper is currently in the range of 13 to 14 Mt, about a third of

which is from Chile. Other large producers are the United States, followed closely by Indonesia and Australia. The most important ore mineral is chalcopyrite  $[\text{CuFeS}_2]$ , and also significant are bornite  $[\text{Cu}_5\text{FeS}_4]$  and chalcocite  $[\text{Cu}_2\text{S}]$ . The first two are primary minerals whereas chalcocite forms principally by their weathering and subsequent reprecipitation of the solubilized Cu as enriched 'blankets' of chalcocite ore beneath the oxidation zone.

Copper ore is predominantly derived from porphyry copper deposits, with lesser but significant contributions from massive sulfide, skarn, and other types of deposits. The host rocks for porphyry copper deposits are felsic granitoid intrusions, and in skarn deposits the intrusions penetrate limestone and associated sedimentary-derived assemblages. The deposits are typically large (commonly hundreds of million tonnes) and of low grade (commonly  $<1\%$  Cu), with successful exploitation dependent mainly on open-pit access and on daily large-tonnage extraction and processing.

World mine production of zinc is about 9 Mt, with almost all of it derived from sphalerite  $[(\text{Zn},\text{Fe})\text{S}]$ , which is also the principal primary source of Cd and several other metals, such as Ge and In. China and Australia are the largest producers, but several other countries mine significant amounts. About half of the annual consumption is for the manufacture of galvanized products to resist corrosion, primarily in the automotive and construction industries.

Mineral-deposit sources of sphalerite are diverse. Large production is obtained chiefly from skarn (e.g., Atamina, Peru), from volcanogenic massive sulfide deposits in which pyrite is the predominant mineral (e.g., Kidd Creek and Brunswick No. 12, Canada) from sedimentary-exhalative (SEDEX) deposits in which layers of Pb, Zn, and Fe sulfides were deposited in fine-grained clastic sedimentary rocks (e.g., Broken Hill and Mt. Isa, Australia), and from Mississippi Valley-type deposits, in which sphalerite and galena  $[\text{PbS}]$  were deposited in large amounts in

cavities, breccias, and as replacements of calcareous sedimentary rocks consisting predominantly of limestone (e.g., Viburnum Trend, U.S.A.).

Whereas sphalerite is the principal mineral source of Zn, galena is the main source of Pb. Annual world mining production of lead is about 3 Mt, and annual consumption is >6 Mt, with the difference made up by recycling. The largest primary producers are China and Australia, and the largest consumers are the European Union and the United States. About 75% of lead consumption is for the manufacture of lead-acid automotive batteries, which are also the principal source of recycled scrap. Unlike Zn, which is an essential biological trace element, Pb has no similar function and is an important environmental hazard (Kesler, 1994). Processing of Pb and Zn concentrates is almost totally by conventional pyrometallurgical smelting, but the most abundant anthropogenic sources of Pb have been coal combustion and gasoline additives (Kesler, 1994).

### *5.2.3. Precious-metal deposits*

The precious-metal group consists of gold, silver, and the platinum-group elements (PGE). The world's leading producer of gold is South Africa, followed by the United States and Australia. Most mining of gold is done specifically for that metal rather than for a polymetallic assemblage, and most gold is produced from auriferous quartz veins. However, appreciable amounts of gold are recovered from the processing of base-metal ores, especially Cu deposits. A characteristic feature of all types of deposits is that nearly all of the gold occurs as the native metal, commonly with Ag in solid solution and less commonly with small but economically important amounts of Au in solid solution in arsenical pyrite. The traditional method of recovering gold from arsenical pyrite, a type of association that is referred to as refractory gold, is

high-temperature roasting to vaporize the S and As, followed by cyanide leaching of the oxidized residue. Environmental concerns about high-As emissions, or the disposal of the  $\text{As}_2\text{O}_3$  that precipitates from the condensed gases, has led to the increased use of pressurized autoclaves to effect the oxidation step. Another environmental concern has been the use of mercury to recover gold by amalgamation. This practice has been largely discontinued because the effects of mercury poisoning are well known, but a legacy of pollution remains in many areas, and amalgamation on a small scale is still practiced by artisan miners in countries such as Brazil and Indonesia.

Gold in recent years has found increased markets in electrical and electronic applications, but these account for <5% of annual consumption. About 90% of the annual production is utilized for jewelry and arts purposes.

Mexico, Peru, and the United States are the largest producers of silver, whose main usage is in photography, plating, jewelry, and electronic and electrical applications. More than three-quarters of the world annual production of silver is obtained from deposits in which base metals or gold are the principal product. For example, the world's largest silver producer is the metamorphosed, stratabound Cannington deposit in Australia. The deposit is of the Broken Hill type and contains about 44 Mt grading 11.6% Pb, 4.4% Zn, and 538 g/t Ag (Walters and Bailey, 1998). The dominant sulfide assemblage is galena-sphalerite-pyrrhotite, and the high Ag content is related mainly to the presence of argentiferous galena and freibergite  $[(\text{Ag,Cu,Fe})_{12}\text{Sb}_4\text{S}_{13}]$ .

Mexico, the leading silver producer by country, obtains about half of its output from mines in which silver is the principal ore metal. Many of the mines are epithermal fissure veins, and most host a polymetallic assemblage whose exploitation is economically dependent on the high Ag values. Although acanthite  $[\text{Ag}_2\text{S}]$  and native silver predominate in some veins, in others much of the Ag occurs in Ag sulfosalts and as Ag substitutions in tetrahedrite

$[(\text{Cu,Fe,Ag})_{12}\text{Sb}_4\text{S}_{13}]$  and other minerals.

The platinum-group metals consist of ruthenium, rhodium, palladium, osmium, iridium, and platinum. Each of the metals occurs naturally in its native form, and in economically exploitable deposits the elements occur overwhelmingly as individual platinum-group mineral (PGM) species. Mutual substitution of the various PGE is common, but substitutions in other minerals, such as base-metal sulfides, typically occurs to only a limited extent. A comprehensive review of PGM and PGE geochemistry is given in Cabri (2002).

The platinum-group metals are generally grouped with gold and silver as precious-metal commodities, but the platinum-group metals have little in common with the other precious metals in terms of their primary geological host-rock associations. The world's largest producer of platinum and rhodium is South Africa, with most of the metal obtained from mines that exploit thin (centimeters rather than meters), PGM-rich layers (averaging  $<10$  g/t PGE) in the Bushveld complex, a layered mafic intrusion that is also a principal source of chromium and vanadium. Platinum and palladium account for all but a very small percentage of world PGE production. Whereas the Bushveld complex accounts for more than a quarter of world palladium production, more than double that amount is obtained as a byproduct from Cu-Ni mines in layered intrusive complexes such as those at Sudbury, Canada, and Noril'sk – Talnakh, Russia; the latter is the world's largest primary source of palladium.

Braggite  $[(\text{Pt,Pd})\text{S}]$ , cooperite  $[\text{PtS}]$ , sperrylite  $[\text{PtAs}_2]$ , and Pt-Fe alloys are among the principal sources of PGE in the Bushveld complex. Michenerite  $[\text{PdBiTe}]$ , moncheite  $[\text{PdTe}_2]$ , and sperrylite are common sources of PGE in some of the Sudbury ores, and all of the above minerals and many more have been reported to occur in the Noril'sk deposits (Cabri, 1981).

The principal consumption of PGE is as a catalyst, especially the use of platinum, or the

more favored palladium because of its superior high-temperature performance, in catalytic converters in motor vehicles. Among the diverse other chief uses are electrical and electronic applications, jewelry, fabrication of laboratory equipment, and dental repairs.

#### *5.2.4 Uranium deposits*

Canada and Australia are the world's largest producers of uranium. All Canadian production is from rich deposits in the Athabasca basin of northern Saskatchewan; among those is the McArthur River mine, which has the world's largest high-grade deposit, estimated at 152,000 t of U from ore grading 15-18% U. These 'unconformity'-type Saskatchewan deposits, which are also the principal deposit-type for Australian uranium production, contain mainly uraninite  $[\text{UO}_2]$  with associated coffinite  $[\text{U}(\text{SiO}_4)_{1-x}(\text{OH})_{4x}]$  and brannerite  $[(\text{U},\text{Ca},\text{Y},\text{Ce})(\text{Ti},\text{Fe})_2\text{O}_6]$  (Plant et al., 1999). The chief uses of uranium are in nuclear power plants and weaponry.

#### *5.2.5. Diamond deposits*

World annual production of natural diamonds, the cubic form of carbon, is about 110 million carats (1 carat = 200 mg). Almost all is derived from kimberlite or its weathered remnants, but Australian production is from the Argyle mine, at which the host rock is lamproite. Kimberlites are olivine- and volatile-rich potassic ultrabasic rocks of variable geological age that typically form near-vertical carrot-shaped 'pipes' intruded into Archean cratons. The volatile-rich component is predominantly  $\text{CO}_2$  in the carbonate minerals calcite and dolomite, and the texture is characteristically inequigranular, with large grains (macrocrysts), usually of olivine  $[\text{Mg}_2\text{SiO}_4]$ , in a fine-grained, olivine-rich matrix.

Australia, Botswana, Russia, and the Democratic Republic of Congo, in decreasing order, account for about 80% of the carats produced annually. In terms of value, however, Australia is surpassed by several countries; for example, South African production in carats is fifth-ranked and is only 40% of that of Australia, but the value is triple that of Australia's diamonds.

#### *5.2.6. Other deposits*

Table 3 summarizes data on the principal sources and uses of numerous other metals. The listing is not intended to be comprehensive.

### 5.3. SULFIDE OXIDATION AND THE GENERATION OF OXIDATION PRODUCTS

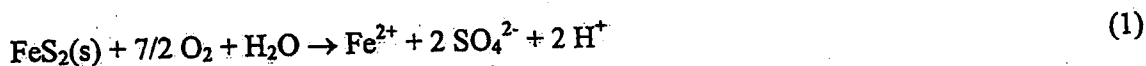
A principal environmental concern associated with mine wastes results from the oxidation of sulfide minerals within the waste materials and mine workings, and the transport and release of oxidation products. The principal sulfide minerals in mine wastes are pyrite and pyrrhotite, but others are susceptible to oxidation, releasing elements such as Al, As, Cd, Co, Cu, Hg, Ni, Pb and Zn to the water flowing through the mine waste.

#### *5.3.1 Pyrite Oxidation*

Pyrite is commonly associated with coal and metal ore deposits. Pyrite oxidation and the factors affecting the kinetics of oxidation ( $O_2$ ,  $Fe^{3+}$ , temperature, pH,  $E_h$  and the presence or absence of microorganisms) have been the focus of extensive study because of their importance in both environmental remediation and mineral separation by flotation (Buckley and Woods, 1987; Brown and Jurinak, 1989; Evangelou and Zhang, 1995; McKibben and Barnes, 1986; Moses et al., 1987; Nordstrom, 1982; Weirsmas and Rimstidt, 1984; Luther, 1987; Williamson

and Rimstidt 1994; Sasaki et al., 1995). Reviews of pyrite oxidation and the formation of acid mine drainage are given by Lawson (1982), Evangelou (1995), Evangelou and Zhang (1995), Nordstrom and Southam (1997), and Nordstrom and Alpers (1999a).

The oxidation of pyrite can occur when the mineral surface is exposed to an oxidant and water, either in oxygenated or anoxic systems, depending on the oxidant. The process is complex and can involve chemical, biological and electrochemical reactions. The chemical oxidation of pyrite can follow a variety of pathways involving surface interactions with dissolved  $O_2$ ,  $Fe^{3+}$  and other mineral catalysts (e.g.,  $MnO_2$ ). Oxidation of pyrite by atmospheric oxygen produces one mole of  $Fe^{2+}$ , two moles of  $SO_4^{2-}$  and two moles of  $H^+$  for every mole of pyrite oxidized (Nordstrom, 1982):



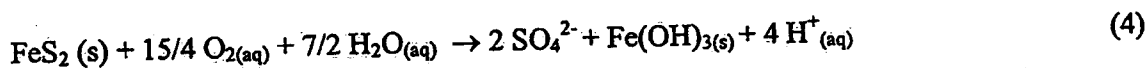
The  $Fe(II)$  thus released may be oxidized to  $Fe(III)$ :



$Fe(III)$  oxyhydroxides such as ferrihydrite (nominally  $5Fe_2O_3 \cdot 9H_2O$ ) may precipitate:



where  $Fe(OH)_3$  is a surrogate for ferrihydrite. Adding equations 1, 2 and 3 yields the overall reaction:



This overall reaction results in the release of 4 moles of  $H^+$  for each mole of pyrite oxidized.

#### 5.3.1.1 Mechanism of pyrite oxidation by $Fe^{3+}$ and $O_2$

Initially pyrite oxidation involves the adsorption of  $O_2$  and water to the partly protonated pyrite surface by bonding to  $Fe^{2+}$  (Fornasiero et al., 1994). Various  $Fe$  oxyhydroxide intermediate



products can form on the pyrite surface, depending on pH. Singer and Stumm (1970) suggested that, under acidic conditions, the major oxidant of pyrite is  $\text{Fe}^{3+}$ , whereas  $\text{O}_2$  becomes the predominant oxidant at circumneutral pH because of the diminished solubility of  $\text{Fe}^{3+}$ . Pyrite oxidation by  $\text{Fe}^{3+}$  at circumneutral pH has also been observed (Brown and Jurinak, 1989; Evangelou and Zhang, 1995; Moses et al., 1987), but the reaction cannot be sustained without the presence of dissolved  $\text{O}_2$  to perpetuate the oxidation to  $\text{Fe}^{3+}$ . When  $\text{O}_2$  is the oxidant under near-neutral pH conditions, one O atom in the sulfate is derived from dissolved  $\text{O}_2$ , with the remainder derived from  $\text{H}_2\text{O}$ . Under acidic conditions, all four O atoms in sulfate are derived from  $\text{H}_2\text{O}$  (Reedy et al., 1991). Although both  $\text{Fe}^{3+}$  and oxygen can bind chemically to the surface, the more rapid oxidation rates for  $\text{Fe}^{3+}$  compared to those for  $\text{O}_2$  are due to a more efficient electron transfer for  $\text{Fe}^{3+}$  (Luther, 1987). A molecular orbital model proposed by Luther (1987) is consistent with pyrite oxidation data obtained by McKibben and Barnes (1986), Moses et al. (1987) and Weirsmas and Rimstidt (1984).

Rate data from the literature for the reaction of pyrite with dissolved  $\text{O}_2$  were compiled by Williamson and Rimstidt (1994) to produce a rate law that is applicable for more than four orders of magnitude in  $\text{O}_2$  concentration and over a pH range of 2 to 10:

$$R = 10^{-8.19(\pm 0.04)} \frac{m_{\text{DO}}^{0.5(\pm 0.04)}}{m_{\text{H}^+}^{0.11(\pm 0.01)}} \quad (5)$$

where  $R$  is the rate of pyrite dissolution in units of  $\text{mol m}^{-2} \text{s}^{-1}$ .

A series of batch and mixed flow reactor experiments was performed at  $\text{pH} < 3$  to determine the effect of  $\text{SO}_4^{2-}$ ,  $\text{Cl}^-$ , ionic strength, and dissolved  $\text{O}_2$  on the rate of pyrite oxidation by  $\text{Fe}^{3+}$ . Of these, only dissolved  $\text{O}_2$  had any appreciable affect on the rate of pyrite oxidation in the presence of  $\text{Fe}^{3+}$ . Williamson and Rimstidt (1994) combined their experimental results with

kinetic data reported from the literature to formulate rate laws that are applicable over a range spanning six order of magnitude in  $\text{Fe}^{3+}$  and  $\text{Fe}^{2+}$  concentrations, and for a pH range of 0.5 to 3.0, when fixed concentrations of dissolved  $\text{O}_2$  are present:

$$R = 10^{-6.07( \pm 0.57)} \frac{m_{\text{Fe}^{3+}}^{0.93( \pm 0.07)}}{m_{\text{Fe}^{2+}}^{0.40( \pm 0.06)}} \quad (6)$$

where  $R$  is the rate of pyrite dissolution in units of  $\text{mol m}^{-2} \text{s}^{-1}$ .

A wide variation in empirical rate laws has been developed to describe pyrite oxidation. The wideness of the range could be due to several factors, among which are differences in sample preparation, different ratios of surface area to volume, and the presence of impurities in the pyrite or in solution. Activation energies determined for pyrite oxidation range from  $50 \text{ kJ mol}^{-1}$  for pH 2 to 4 to  $92 \text{ kJ mol}^{-1}$  for pH 6 to 8, regardless of whether dissolved  $\text{O}_2$  or  $\text{Fe(III)}$  is used as the oxidant (Nicholson, 1994; Weirsmas and Rimstidt, 1984). Table 4 provides a summary of the proposed rate expressions for the dissolution of pyrite in solutions containing dissolved  $\text{O}_2$  and  $\text{Fe(III)}$ . Activation energies are observed to be higher for pH values in the range of 6 to 8 than in the range from 2 to 4. Casey and Sposito (1991) suggested that the proton adsorption/desorption reactions can contribute up to  $50 \text{ kJ mol}^{-1}$  to the experimental activation energy of dissolution reactions for silicate minerals. The hydrogen-ion activity or pH, therefore, may play an important role in the observed activation energy for the oxidation of sulfide minerals. Regardless, the high activation energies observed indicate that the rate-limiting step in pyrite oxidation is related to electron transfer at the pyrite surface.

Holmes and Crundwell (2000) studied the kinetics of pyrite oxidation and reduction independently using electrochemical techniques. The kinetics of the half reactions are related to the overall dissolution reaction assuming no accumulation of charge on the surface. This

assumption was used to derive expressions for the mixed potential and rate of dissolution, which agreed with those obtained by McKibben and Barnes (1986) and Williamson and Rimstidt (1994). The results showed that the electrochemical reaction steps occurring at the mineral – solution interface control the rate of dissolution.

### *5.3.2 Pyrrhotite Oxidation*

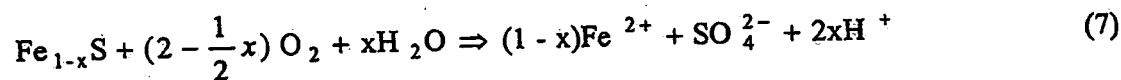
Pyrrhotite is a common Fe-sulfide mineral. Although there have been numerous studies of the oxidation of pyrite, fewer studies have focused on pyrrhotite oxidation (Buckley and Woods, 1985; Jones et al., 1992; Nicholson and Scharer, 1994; Pratt et al., 1994a,b; Thomas et al., 1998; Janzen et al., 2000). The pyrrhotite structure is based on hexagonal close packing, but is disordered (i.e., NiAs-type structure), giving rise to nonstoichiometric and stoichiometric compositions in which  $x$  in the formula  $\text{Fe}_{1-x}\text{S}$  can vary from 0.125 ( $\text{Fe}_7\text{S}_8$ ) to 0 ( $\text{FeS}$ ). The Fe vacancies within the structure may be charge-compensated by  $\text{Fe}^{3+}$  (Vaughan and Craig, 1978) or an approximation thereof. Analyses of cleaved pyrrhotite surfaces under vacuum showed Fe(III)-S interactions on the pyrrhotite surface (Pratt et al., 1994a). The deficiency in Fe within the pyrrhotite structure can result in a symmetry that varies from monoclinic ( $\text{Fe}_7\text{S}_8$ ) to hexagonal ( $\text{Fe}_{11}\text{S}_{12}$ ), with the composition progressing to stoichiometric troilite ( $\text{FeS}$ ). Orlova et al. (1988) examined the reaction rates for monoclinic and hexagonal pyrrhotite and concluded that the hexagonal form was the more reactive.

The deficiency of Fe in the pyrrhotite structure may affect the oxidation behavior. Nicholson and Scharer (1994) observed a dependency of activation energy on pH; the energy ranged from 52-58  $\text{kJ mol}^{-1}$  at pH 2 to 4, and almost doubled to 100  $\text{kJ mol}^{-1}$  at circumneutral pH (i.e., 6). These values are similar to activation energies noted for pyrite, suggesting a chemical-controlled

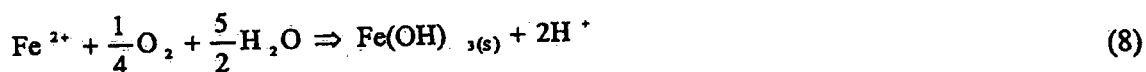
reaction. Orlova et al. (1988) observed a range of activation energies for both monoclinic and hexagonal varieties ranging from 50 to 46 kJ mol<sup>-1</sup>, respectively. It was argued that the lower activation energy was significant to the hexagonal variety. Janzen et al. (2000), however, did not observe consistent trends between activation energy and crystal structure.

#### 5.3.2.1 Chemical oxidation by O<sub>2</sub> and Fe<sup>3+</sup>

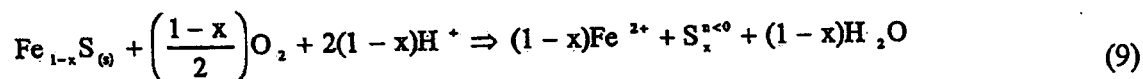
Pyrrhotite dissolution can proceed through oxidative or non-oxidative reactions. Oxidative dissolution can be at least 10<sup>3</sup> times slower than non-oxidative reactions (Thomas et al., 1998). Dissolved O<sub>2</sub> and Fe<sup>3+</sup> can be important oxidants of pyrrhotite. When oxygen is the primary oxidant, the overall reaction may be written as:



The production of protons is linked to the mineral stoichiometry. Up to one-quarter mole of the protons produced are derived from the oxidation of one mole of the Fe-deficient form ( $x = 0.125$ ), whereas no protons are produced from the stoichiometric form, which is troilite ( $x = 0$ ). The release of protons can also result from the oxidation of the dissolved Fe resulting from the precipitation of ferric hydroxide:



In other circumstances, the oxidation reactions may not proceed to completion. Partial oxidation may result in only a small proportion of the S being transformed to sulfate, with the remainder accumulating as reduced sulfur species (polysulfides and elemental sulfur) at the mineral surface (Janzen et al., 2000).



The rates of oxidation of both pyrite and pyrrhotite at 25 °C and standard atmospheric oxygen indicate that pyrrhotite can react 20-100 times faster than pyrite. During oxidation of a particle of pyrrhotite, Fe diffuses to the exposed surface, thereby creating a S-enriched inner zone that contains disulfide and polysulfide-like species (Mycroft et al., 1995).

#### 5.3.2.2 Non-oxidative mechanism

Non-oxidative dissolution of pyrrhotite occurs in acidic solutions when predominant  $\text{S}^{2-}$  surface species are exposed. The reaction occurs as:



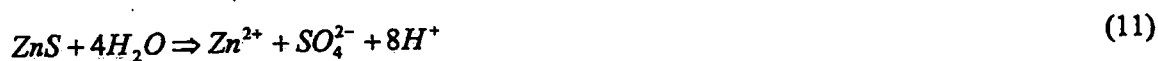
Jones et al. (1992) observed restructuring of sulfur-rich pyrrhotite surfaces in deoxygenated acid, resulting in the development of a surface dominated by a discontinuous layer of a tetragonal intermediate  $\text{Fe}_2\text{S}_3$  structure. Janzen et al. (2000) showed a significant release of  $\text{Fe}^{2+}$  from pyrrhotite in acidic solutions in which oxygen was not present. Although  $\text{Fe}^{2+}$  concentrations increased linearly with time, sulfate values remained unchanged, with sulfur from pyrrhotite dissolution remaining in a reduced state ( $\text{S}^{2-}$ ). Thomas et al. (1998, 2001) proposed a dissolution mechanism that allows two distinct pathways: a) Fe leaves the surface, with no additional electrons released from the structure, and b) after a critical accumulation of charge, reduction of polysulfide to sulfide occurs, resulting in the release of negative charge from the surface in the form of  $\text{HS}^-$ . The significant feature of this process is the delay between the release of  $\text{Fe}^{2+}$  and  $\text{HS}^-$ .

### 5.3.3 Oxidation of Other Metal Sulfides

#### 5.3.3.1 Sphalerite

The oxidation of sphalerite is dependent on a number of factors, among which are the concentration of oxidants, such as dissolved  $O_2$  or  $Fe(III)$  in solution, the temperature, and the pH (Bobeck and Su, 1985; Crundwell, 1988; Olanipekun, 1999; Perez and Dutrizac, 1991; Rimstidt et al., 1994). For sphalerite, Vaughan and Craig (1978) reported a solubility product of  $K_{sp}=1 \times 10^{-20.6}$  at 25 °C in water. Other researchers have reported similar values (Daskalakis and Helz, 1993).

For sphalerite in dilute  $Fe(III)$  solutions, Rimstidt et al. (1994) obtained a dissolution rate of  $7.0 \times 10^{-8} \text{ mol m}^{-2}\text{s}^{-1}$  with a corresponding activation energy of  $27 \text{ kJ mol}^{-1}$  over a range of 25-60 °C. The concentration of  $Fe(III)$  used was  $10^{-3} \text{ M}$ , which is similar to dissolved Fe concentrations ( $2.9 \times 10^{-3} \text{ M}$ ) typically observed in acidic mine waters (Lin, 1997). The overall oxidation reaction for pure sphalerite, assuming that all sulfur is oxidized to sulfate, is:



XPS examination of oxidized sphalerite showed the development of a surface layer of metal-deficient sulfide (Buckley et al., 1989) whose formation in acid solution is described by:



Weisener et al. (2001, 2002) observed increased rates of oxidation and increased acid consumption as a function of the amount of solid-solution Fe in sphalerite  $[(Zn,Fe)S]$ . Apparent activation energies of  $21\text{-}28 \text{ kJ mol}^{-1}$  obtained at 25-85 °C are similar to the values reported by Rimstidt et al. (1994). Weisener et al. (2001, 2002) suggested that the production of polysulfide species results in a lower diffusion gradient at the mineral surface, thus leading to lower

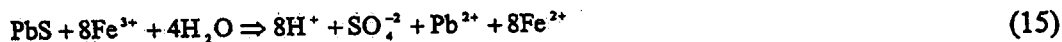
reactivity with potential oxidants and to diffusion-limited release of Zn and Fe from the bulk mineral. Elemental sulfur was not observed to limit the reactivity of the mineral-surface. The accumulation of polysulfides and  $S^0$  on the sphalerite surface under oxygenated conditions can affect the acid-neutralization capacity because the polysulfides and  $S^0$  consume acid when pH is  $<3$ . The resulting formation of a S-enriched surface slows the subsequent rate of dissolution of sphalerite in the absence of bacteria. Under these conditions  $S^0$  does not passivate the surface (Weisener, 2002).

#### 5.3.3.2 Galena and chalcopyrite

Galena and chalcopyrite are commonly associated with acid-generating minerals, such as pyrite and pyrrhotite. Acid ferric sulfate solutions, generated through the oxidation of Fe sulfides can enhance the oxidation of Pb- and Cu-bearing sulfide minerals. The oxidation of galena has been studied by Buckley and Woods (1984a), Tossell and Vaughan (1987), Fornasiero et al. (1994), Kim et al. (1995), Prestidge et al. (1995), Basilio et al. (1996), Kartio et al. (1996, 1998), Chernyshova and Andreev (1997), Jennings et al. (2000), Nowak and Laajalehto (2000), Shapter et al. (2000), and others. XPS studies showed that  $S^0$  formed when galena was oxidized in a hydrogen peroxide solution, and that metal-deficient surfaces resulted from oxidation by dilute acetic acid solutions (Buckley and Woods, 1984a). In natural oxygenated environments, galena will weather to anglesite, which is weakly soluble below pH 6 (Lin, 1997; Shapter et al., 2000):



Galena may also be oxidized by Fe(III) under acidic conditions (Rimstidt et al., 1994):



The oxidation of galena in air may result in the formation of lead hydroxide and lead oxide (Evans and Raftery, 1982; Buckley and Woods, 1984a; Laajalehto et al., 1993). Oxidation in aqueous solutions may lead to the formation of lead oxides and lead sulfate surface products (Fornasiero et al., 1994; Kartio et al., 1996; Kim et al., 1995; Nowak and Laajalehto, 2000). In the absence of oxygen, both Pb and sulfide ions are released to solution in the form of free Pb ions and hydrogen sulfide (Fornasiero et al., 1994). Jennings et al. (2000) showed that galena was not acid-generating when exposed to accelerated oxidation using hydrogen peroxide. This reaction resulted in the accumulation of anglesite on the mineral surface.

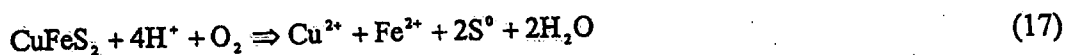
XPS study by Buckley and Woods (1984b) showed that freshly fractured chalcopyrite surfaces exposed to air formed a ferric oxyhydroxide overlayer with a Fe-deficient region composed of  $\text{CuS}_2$ . Acid-treated surfaces of fractured chalcopyrite showed an increase in the thickness of the  $\text{CuS}_2$  layer and the presence of elemental sulfur. Hackl et al. (1995) suggested that dissolution of chalcopyrite is passivated by a thin ( $<1 \mu\text{m}$ ) Cu-rich surface layer which forms as a result of solid-state changes. The passivating surface layer consists of Cu polysulfide,  $\text{CuS}_n$ , where  $n = >2$ . Hackl et al. (1995) described the dissolution kinetics as a mixed diffusion and chemical reaction whose rate is controlled by the rate at which the Cu polysulfide is leached. The oxidation of chalcopyrite in the presence ferric ions under acidic conditions can be expressed as:



Hiroyoshi et al. (1997) monitored the oxygen consumption, sulfur formation, total Fe, and Fe(II) concentrations at different pH levels during the oxidation of chalcopyrite. On the basis of the



reaction products formed, it was concluded that ferrous ions catalyzed the oxidation by dissolved oxygen in acidic media:



This conclusion agrees with the observation and interpretations made from testing monomineralic chalcopyrite with peroxide solution; acid production was not observed. Chalcopyrite can be acid-consuming via the production of  $\text{S}^0$  (Smart et al., 2001).

The dissolution of chalcopyrite can be also be influenced strongly by galvanic effects. The presence of pyrite or molybdenite in association with chalcopyrite can cause accelerated rates of chalcopyrite dissolution (Dutrizac and MacDonald, 1973), whereas the presence of Fe-rich sphalerite and galena can slow the dissolution.

#### *5.3.1.4 Arsenic and mercury sulfides*

The oxidation of arsenopyrite [ $\text{FeAsS}$ ] releases both S and As. Buckley and Walker (1988) studied the oxidation of arsenopyrite in alkaline and in acidic aqueous solutions. In air, the mineral reacted rapidly, and the oxidation of As to As(III) was more rapid than the oxidation of Fe on the same surface. Only a small amount of sulfur oxidation occurred. Under acidic conditions, the mineral formed S-rich surfaces.

Nesbitt et al. (1995) conducted a detailed study of the oxidation of arsenopyrite in oxygenated solutions. Arsenic and S were observed to exist in multiple oxidation states near the pristine surface. After reaction with air-saturated distilled water, Fe(III) oxyhydroxides formed the dominant Fe surface species, and As(V), As(III), and As(I) were as abundant as As(-I) surface species. An appreciable amount of sulfate was observed on the mineral surface. Arsenic was more readily oxidized than S, and similar rates of the oxidation of As(-I) and  $\text{Fe(II)}^+$  surface

species were observed. Nesbitt et al. (1995) concluded that continued diffusion of As to the surface under these conditions can produce large amounts of  $\text{As}^{3+}$  and  $\text{As}^{5+}$ , promoting rapid selective leaching of arsenites and arsenates.

Rimstidt et al. (1994) measured the rate of reaction of arsenopyrite under conditions typical of acid mine drainage environments. Arsenopyrite was observed to be more reactive than pyrite, chalcopyrite, galena, and sphalerite. Oxidation of arsenopyrite led to the formation of scorodite on the surface. The activation energies for arsenopyrite oxidation varied from  $18 \text{ kJ mol}^{-1}$  at 0 to  $25^\circ\text{C}$ , to a slightly negative  $E_a$  of  $-6 \text{ kJ mol}^{-1}$  from 25 to  $60^\circ\text{C}$ . Rimstidt et al. (1994) attributed the negative activation energies to competition between the dominant reactions that occur at all temperatures and the less vigorous side-reactions that contribute to rate-limiting behavior at higher temperatures.

An investigation of the surface composition and chemical state of three naturally weathered arsenopyrite samples exposed for periods ranging from 14 days to 25 years showed that the arsenopyrite surface has an effective passivating layer that protects the mineral from further oxidation (Nesbitt and Muir, 1998). The same samples were then reacted with mine-waste waters, which caused extensive leaching of the arsenopyrite surface below the oxidized overlayers. The acidic nature of the solution caused dissolution of the previously accumulated ferric arsenite and arsenate salts.

Foster et al. (1998) provided a detailed comparison of the oxidized speciation and local geometry of As for three California mine-waste materials: fully oxidized tailings, partly oxidized tailings, and roasted sulfide ore. The fully oxidized tailings showed As(V) species sorbed primarily on the ferric oxyhydroxides and aluminosilicates. The partly oxidized tailings contained equal amounts of arsenopyrite and arsenian pyrite that accounted for 20% of the total

As, and the remaining 80% consisted of  $\text{As}^{5+}$  as a precipitate of scorodite. The roasted sulfide ore contained an As(V) species that had substituted for sulfate in jarosite  $[\text{KFe}_3(\text{SO}_4)_2(\text{OH})_6]$  and was sorbed onto the surfaces of hematite and ferric oxyhydroxide grains.

Cinnabar  $[\text{HgS}]$ , the principal ore of mercury, is the most thermodynamically stable form at low temperature (Benoit et al., 1999; Barnett et al., 2001). The presence of trace impurities, such as Zn, Se, and Fe, can impede the conversion of metacinnabar, which is the high-temperature form, to cinnabar. The trace impurities decrease the inversion temperature and thus retard the conversion (Barnett et al., 1997). Therefore, in some environments the availability of impurities will favor the *in-situ* formation of metacinnabar over cinnabar. The formation of  $\text{HgS}$  is favored under reducing conditions, in part because of the high affinity of Hg compounds for S. Cinnabar is kinetically resistant to oxidation, and can remain in soil and tailing impoundments even under oxidizing conditions (Barnett et al., 1997). Although little has been published on its oxidation rates in soils, the observed persistence of  $\text{HgS}$  in soils at minesites suggests that its weathering is slow under typical oxidative environments (Barnett et al., 1997; Gray et al., 2000).

### *5.3.2 Bacteria and Sulfide-Mineral Oxidation*

#### *5.3.2.1 Organisms that catalyze sulfide oxidation*

Microorganisms contribute to a vast array of biogeochemical cycles, among which are oxygenic photosynthesis, ammonia oxidation, sulfur oxidation/reduction, methanogenesis, fermentation, and respiration. This diversity allows microorganisms to survive in environments that have finite nutrients and low pH, as occur in acidic mine effluents. Bacteria are among the few forms of life that can tolerate these extreme environments. Chemolithotrophs are microorganisms that derive their energy requirements from inorganic sources in the presence of

oxygen. Some chemolithotrophs can substitute nitrate or ferric iron as the electron acceptor if oxygen is unavailable. The genera *Thiobacillus*, *Acidothiobacillus*, and *Leptospirillum* contain numerous species that can utilize various sulfur compounds (Table 5). This group of organisms is largely responsible for the oxidation of sulfide minerals and includes Fe- and S-oxidizing bacteria. A detailed historical review of the isolation and identification of these microorganisms is provided by Nordstrom and Alpers (1999a).

Sulfur can exist in several oxidation states in nature, the most common being sulfide (-2), polysulfides ( $-2 < x < 0$ ), elemental sulfur (0), and sulfate (+6). Sulfur oxidizers commonly occur within interfaces of low-energy environments, where anoxic waters mix slowly with oxic conditions above. Acidophilic sulfide-oxidizing bacteria are commonly isolated from acid mine drainage environments in which abundant sources of sulfur from sulfide-rich material, such as waste rocks and tailing impoundments, are available. The availability of oxygen in conjunction with an abundant source of S supports bacterial growth and activity. Bacterial catalysis of the available sulfide minerals accelerates the transformation of the reduced compounds to sulfate. The subsequent low pH produced, typically  $< 4$ , allows the acidophilic organisms to thrive where other organisms are excluded. Neutral-pH oxidizers of S include several *Thiobacillus* species. *Thiobacillus thioparus* is a mesophilic bacterium with an optimum pH range between 6.0 and 8.0. *T. thioparus* can oxidize sulfide, thiosulfate, and other reduced species of S (Gould, 1994).

*Acidothiobacillus thiooxidans*, formerly known as *Thiobacillus thiooxidans*, is an acidophilic bacterium that oxidizes  $S^0$  and thiosulfate, but not Fe. Due to the rapid kinetics involved in sulfide oxidation by dissolved oxygen, some sulfide-oxidizing bacteria are in continuous competition with the chemical oxidation mechanism. *Acidothiobacillus ferrooxidans*, formerly known as *Thiobacillus ferrooxidans*, is capable of utilizing Fe(II),  $S^0$ , or sulfide minerals as a

source of energy for metabolic activity and plays an important role in the biogeochemical cycling of Fe and S. *Leptospirillum ferrooxidans* is metabolically similar to *A. ferrooxidans* but morphologically differs in having a spherical structure and a preferred pH range of 1.5 to 2.1. *L. ferrooxidans* lacks the capacity to oxidize sulfur compounds, preferring the selective oxidation of Fe(II), thus making it less sensitive to Fe(III) inhibition and allowing this organism to thrive at higher redox potentials than *T. ferrooxidans* (Breed and Hansford, 1999).

#### 5.3.2.2 Conditions for optimal growth of bacterial species

The mesophiles *A. thiooxidans* and *A. ferrooxidans* have been found in equal proportions in mine effluents regardless of geological and climatological conditions. The temperature optimum for *A. ferrooxidans* and *A. thiooxidans* lies between 15 and 35 °C. Both are acidophiles and can tolerate a pH range of 1.5-6.0, with optimum growth between pH 2.0 and 2.5. The ability of these microorganisms to adapt and tolerate different pH and metal concentrations makes them effective catalysts for the oxidation of sulfides in mine wastes. *A. ferrooxidans* is an obligate aerobe and has a strict requirement of CO<sub>2</sub> as a source of carbon for growth. The concentration of CO<sub>2</sub> that effectively supports the maximal growth rate has been found to be 7-8%. An increase above 8% results in inhibited growth characteristics (Barron and Lueking, 1990). Both *L. ferrooxidans* and *A. ferrooxidans* occur in similar environments, but *L. ferrooxidans* is more tolerant to extremes in temperature and pH (Edwards et al., 1999).

#### 5.3.2.3 Role of bacteria in generation of acidic drainage

The pre-1991 research involving microbial oxidation of 29 sulfide minerals of Fe, Cu, As, Sb, Ga, Zn, Pb, Ni, and Hg was compiled by Nordstrom and Southam (1997). The importance of microbially-mediated sulfide oxidation has been recognized for several decades (Nordstrom and

Southam, 1997). Bacteria catalyze the oxidative dissolution of sulfide minerals, increasing the production of acidity in mine wastes. In the absence of bacteria, the rate of sulfide oxidation declines as the pH decreases below pH 3.5 (Singer and Stumm, 1970).

Sulfide-mineral oxidation by microbial populations has been postulated to proceed via direct or indirect mechanisms (Tributsch and Bennett, 1981a,b; Boon and Heijnen, 2001; Fowler, 2001; Sand et al., 2001; Tributsch, 2001). In the direct mechanism, it is assumed that the action taken by the attached cell or bacterium on a metal sulfide will solubilize the mineral surface through direct enzymatic oxidation reactions. The sulfur moiety on the mineral surface is oxidized to sulfate without the production of any detectable intermediates. The indirect mechanism assumes that the cell or bacteria do not act directly on the sulfide-mineral surface, but catalyze reactions proximal to the mineral surface. The products of these bacterially catalyzed reactions act on the mineral surfaces to promote oxidation of the dissolved Fe(II) and S<sup>0</sup> that are generated via chemical oxidative processes. Ferrous iron and S<sup>0</sup>, present at the mineral surface, are biologically oxidized to Fe(III) and sulfate. Physical attachment is not required for the bacterial catalysis to occur. The resulting catalysis promotes chemical oxidation of the sulfide-mineral surface, perpetuating the sulfide oxidation process (Figure 1).

The following equations summarize the two mechanisms using pyrite as an example:

Direct interaction:



Indirect interaction:





Dissolved oxygen or Fe(III) ions are considered to be the primary oxidants in either chemical or biologically mediated processes which occur in the environment. The ability of *A. ferrooxidans* to oxidize metal sulfides in the absence of Fe ions has been used as supporting evidence for a direct mechanism (Tributsch and Bennett, 1981a,b). However, *A. ferrooxidans* in the absence of Fe ions can behave in a manner similar to that of *A. thiooxidans*, utilizing the oxidation of S as the metabolic energy source (Figure 2; Sand et al., 2001).

Sand et al. (2001) suggested that Fe(III) ions or protons ( $\text{H}^+$ ) are the only chemical agents that dissolve a metal sulfide, and that bacteria have functions to regenerate these ions and to concentrate them at the mineral/water or the mineral/bacterial cell interface. The chemical reactions take place in a thin layer of glycocalyx surrounding bacterial cells. The concentration of reactants in this nanometer-thick layer causes the observed acceleration of rates of oxidative dissolution of sulfide minerals.

Tributsch (2001) suggested that bacterially mediated oxidation proceeds through mechanisms of cooperative dissolution and contact leaching. Contact leaching replaces the term direct leaching because this definition would require an enzymatic interaction between the bacterial membrane and the cell at the sulfide surface, which is not observed. The production of discrete etch-pit chain sequences observed on pyrite surfaces by *A. ferrooxidans* (Tributsch, 2001) is consistent with the hypothesis of contact leaching. Coordinated microbiological, mineralogical, and geochemical studies conducted at the Kidd Creek tailings impoundment, Timmins, Ontario, suggest that the early stages of sulfide oxidation are catalyzed by neutrophilic bacteria, including *T. thioparus* and related species. After acidic conditions are attained, acidophilic species,

including *A. thiooxidans* and related species, and *A. ferrooxidans* and related species, become established (Blowes et al., 1995).

Recent studies at the Iron Mountain acid mine drainage site in California suggest that the main role of *A. ferrooxidans* is to oxidize Fe downstream from the principal acid-generating site, and that the primary effect is to enhance the precipitation of Fe oxyhydroxides (Banfield and Welch, 2000). Other Fe-oxidizing bacteria (e.g., *L. ferrooxidans*) and archaeal (e.g., *Thermoplasmales*) species have been observed proximal to the sulfide ore (Edwards et al., 2000). The utilization of energy derived from Fe or S oxidation in other prokaryotes remains unclear, but it can be surmised that the mechanism involved could be broadly similar to that determined for *A. ferrooxidans* (Banfield and Welch, 2000).

#### 5.3.2.4 Impact of bacteria on the rate of sulfide-mineral oxidation

The chemical oxidation of metal sulfides is controlled in part by the dissolution of sulfide minerals under acidic conditions and by the presence of oxidants ( $\text{DO}$ ,  $\text{Fe}^{3+}$ ) that lead to the disruption of sulfide chemical bonds. Bacteria can have a significant effect on the rate of oxidative dissolution of sulfide minerals by controlling mineral solubility and surface reactivity. Metal-enriched waters and solutions rich in sulfuric acid that form in association with mining can be directly linked to microbial activity. The majority of studies to date have focused on the reactivity and kinetics of sulfide minerals in the presence of *A. ferrooxidans* and *L. ferrooxidans*, and in some cases *A. thiooxidans* (Singer and Stumm, 1970; Tributsch and Bennett, 1981a,b; Sand et al., 1992, 2001; Nordstrom and Southam, 1997; Sasaki et al., 1998; Edwards et al., 1998, 1999, 2000; Nordstrom and Alpers, 1999a; Banfield and Welch, 2000; Tributsch, 2001).



Additional studies have been conducted on other species of bacteria and archaea (Edwards et al., 1998, 1999, 2000).

Singer and Stumm (1970) determined that in the presence of *A. ferrooxidans* the oxidation of Fe(II) from pyrite increased from  $3 \times 10^{-12} \text{ mol L}^{-1} \text{ s}^{-1}$  to  $\sim 3 \times 10^{-7} \text{ mol L}^{-1} \text{ s}^{-1}$ , almost five orders of magnitude. Nordstrom (1985) measured the Fe-oxidation rates and stream velocities in downstream effluents from mine tailings. The oxidation rates were estimated to be between  $2 \times 10^{-7}$  and  $8 \times 10^{-7} \text{ mol L}^{-1} \text{ s}^{-1}$ , with the range attributed to climatic variations. Table 6 provides a compilation of abiotic, microbial, and field rate-data for pyrite, sphalerite, galena, and chalcopyrite.

In the review by Nordstrom and Southam (1997), insightful correlations among the relationships of grain size, surface area, and microbial leaching rates were provided (taken from Olson, 1991; Southam and Beveridge, 1992). Olson (1991) conducted an inter-laboratory comparison of pyrite bioleaching rates by *A. ferrooxidans* using a standard set of conditions. Evaluation of data collected by Olson determined that the average microbial rate of oxidation for pyrite is  $\sim 8.8 \times 10^{-8} \text{ mol m}^{-2} \text{ s}^{-1}$ . Nordstrom and Alpers (1999a) concluded that, because this rate fell between the abiotic oxidation of pyrite by Fe(III) and the microbial oxidation of Fe(II), little difference was effected by *A. ferrooxidans*. The lower rate of microbial pyrite oxidation compared to the oxidation rate of Fe(II) by *A. ferrooxidans* suggests that the heterogeneous reaction is the rate-determining step (Nordstrom and Alpers, 1999a). Although uncertainties exist regarding rates and the natural variation in the oxidation of Fe(II), the rates are large enough that there is no significant difference. Consequently, the kinetics of pyrite oxidation may be controlled by the rate involved in the production of aqueous ferric iron from ferrous iron via microbial catalysis (Nordstrom and Alpers, 1999a).

## 5.4 ACID NEUTRALIZATION MECHANISMS AT MINE SITES

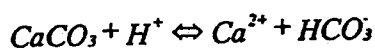
The oxidation of sulfide minerals in mine waste-rock piles and tailings impoundments generates acidic waters containing high concentrations of  $\text{SO}_4$ ,  $\text{Fe(II)}$  and other metals. The water affected by sulfide oxidation is displaced into underlying or adjacent geological materials, or it is discharged directly to the adjacent surface-water flow system. Geochemical reactions with the gangue minerals result in progressive increases in the pore-water pH and the attenuation of some dissolved metals. A sequence of geochemical reactions occurring in the mine wastes and in underlying aquifers results in profound changes in the concentrations of dissolved constituents and in the mineralogy and physical properties of the mine waste and aquifer materials. Low pH conditions promote the dissolution of many metal-bearing solids and the desorption of metals from solid surfaces. Increases in pH through acid-neutralization reactions can lead to pronounced declines in the concentrations of dissolved metals released from mine wastes.

### 5.4.1 Mechanisms of Acid Neutralization

The acid generated through sulfide oxidation reacts with the non-sulfide gangue minerals within the mine wastes. The most significant pH-buffering reactions in mine settings are the dissolution of carbonate minerals, aluminum hydroxide and ferric oxyhydroxide minerals, and aluminosilicate minerals.

#### 5.4.1.1 Carbonate-mineral dissolution

The most abundant carbonate minerals in mine wastes are calcite [ $\text{CaCO}_3$ ], dolomite [ $\text{CaMg}(\text{CO}_3)_2$ ], ankerite [ $\text{Ca(Fe,Mg)}(\text{CO}_3)_2$ ], siderite [ $\text{FeCO}_3$ ] or mixtures thereof. The dissolution of calcite can be described as:



[23]

or, at low pH, as



[24]

Dissolution of carbonate minerals has the potential to raise the pH of the pore water to near neutral. Dissolution of carbonate minerals releases Ca, Mg, Mn, Fe, and other cations that are as solid-solution substitutions or as impurities, and increases the alkalinity of the water. At many sites, the mass of carbonate minerals contained in the mine wastes exceeds that of the sulfide minerals, and the rapid dissolution of carbonate minerals is sufficient to maintain neutral pH conditions through the mines or their waste piles. Neutral pH conditions have been observed in tailings impoundments derived from processing carbonate-bearing vein-type gold deposits (Blowes, 1990; McCreadie et al., 2000), and in open pits derived from gold mining (Shevenell et al., 1999).

Many mines and mine wastes derived from massive sulfide ore deposits contain a sulfide content in excess of the carbonate neutralization capacity. At these sites, the available carbonate content is completely consumed, with the most soluble and most reactive carbonate minerals depleted first. Calcite is depleted initially, followed by dolomite-ankerite and siderite (Blowes and Ptacek, 1994). As the carbonate content of the waste dissolves, the pH is buffered to near neutral. The depletion of carbonate minerals through consumption by acid-neutralization reactions has been documented for a number of settings, including base-metal mine tailings impoundments (Dubrovsky et al., 1984; Dubrovsky, 1986; Blowes and Jambor, 1990; Johnson et al., 2000), aquifers impacted by drainage from mine wastes (Morin et al., 1988), and coal-mine spoils (Cravotta, 1994). In these studies, the greatest depletion occurs at the advancing acid front. An abrupt increase in solid-phase carbonate concentration is observed, suggesting that the dissolution of carbonate minerals is rapid. Measurements of the carbonate content of mine

wastes, in front of and behind the carbonate dissolution front, indicate that carbonate depletion occurs over a small distance along the path of groundwater flow, and that carbonate minerals are absent behind the acid front (Dubrovsky et al., 1984; Johnson et al., 2000). Detailed laboratory column studies conducted by Jurjovec et al. (2002, 2003) confirmed that the depletion of carbonate minerals in response to an advancing acid front is rapid. Jurjovec et al. (2002, 2003) observed stable pH conditions while alkalinity and cations were produced through carbonate dissolution, followed by a pronounced drop in pH after carbonate minerals were depleted (Figure 3).

The solubility products for the dissolution of calcite, dolomite-ankerite, and siderite vary, with calcite having the highest solubility product and siderite the lowest (Table 7). Field observations suggest that dissolution of the most soluble of these minerals will proceed first, followed by dissolution of the next most soluble mineral. As Fe-sulfide minerals oxidize, Fe(II) can be released to anoxic pore waters and can react with the  $\text{HCO}_3^-$  produced through calcite dissolution, thereby forming siderite. Observations from field sites, coupled with geochemical modelling results, suggest that secondary siderite does form through this reaction (e.g., Ho et al., 1984; Morin et al., 1988; Blowes and Jambor, 1990; Ptacek and Blowes, 1994). Al et al. (2000) identified secondary siderite on calcite surfaces, consistent with theoretical predictions. In laboratory studies conducted by Jurjovec et al. (2002, 2003), dissolution of various carbonate minerals, including calcite, dolomite-ankerite, and siderite could not be distinguished. Under the near-neutral pH conditions maintained by carbonate-mineral dissolution, the precipitation of crystalline and amorphous metal hydroxides is favored. Cations released through sulfide oxidation and the dissolution of carbonate and aluminosilicate minerals can lead to the formation of secondary hydroxide phases that accumulate in the waste solids. These phases may

subsequently dissolve as additional acid is produced through sulfide-mineral oxidation reactions. Dissolution of these secondary minerals contributes to acid neutralization.

#### *5.4.1.2 Dissolution of hydroxide minerals*

After the carbonate minerals are depleted, the pH falls until equilibrium with the most soluble secondary hydroxide mineral is attained. An abrupt increase in the concentration of dissolved Al has been observed to coincide with carbonate depletion at several mine-tailings impoundments. These observations suggest that the initial hydroxide mineral to dissolve is an aluminum hydroxide. Although a discrete Al-bearing phase has not been isolated, it is generally assumed to be amorphous Al hydroxide  $[\text{Al}(\text{OH})_3]$  or gibbsite [crystalline  $\text{Al}(\text{OH})_3$ ]. Dissolution of this Al-bearing phase buffers the pH in the region of 4.0 to 4.5 (Dubrovsky, 1986; Blowes and Jambor, 1990; Johnson et al., 2000). Although repeated attempts have been made, the presence of these Al-bearing phases has not been confirmed through mineralogical studies. After the secondary Al phases present in the tailings are depleted, the pH falls until equilibrium with an Fe-oxyhydroxide mineral, typically ferrihydrite (nominally  $9\text{Fe}_2\text{O}_3 \cdot 5\text{H}_2\text{O}$ ) or goethite ( $\alpha\text{-FeOOH}$ ), has been attained. Dissolution of ferric oxyhydroxide minerals typically maintains pH values in the range of 2.5 to 3.5.

#### *5.4.1.3 Dissolution of aluminosilicate minerals*

Gangue minerals associated with sulfide-rich tailings include various aluminosilicate minerals such as chlorite, smectite, biotite, muscovite, plagioclase, amphibole, and pyroxene. Their contribution to acid-neutralization reactions has been examined in a number of field studies and through controlled laboratory experiments. During the period of carbonate- and hydroxide-

mineral dissolution, aluminosilicate minerals may also dissolve, thus consuming  $H^+$  and releasing  $H_4SiO_4$ ,  $Al^{3+}$ , and other cations, including K, Ca, Mg, and Mn. Aluminosilicate dissolution is generally not rapid enough to buffer the pore water to a specific pH. Such reactions, however, do consume  $H^+$  and contribute to the overall acid-neutralization potential of mine wastes. In addition to  $H^+$  consumption, Al and other metals released from aluminosilicate minerals may accumulate in secondary products such as amorphous  $Al(OH)_3$  or gibbsite that act as secondary pH buffers. As with other phases contributing to acid neutralization, the mass and composition of aluminosilicates vary from site to site and within an individual site.

Detailed field studies conducted at the Heath Steele tailings impoundment, New Brunswick, Canada, illustrate the role of aluminosilicate-mineral dissolution in contributing to acid neutralization. The tailings contain in excess of 85 wt.% sulfide minerals, where partial oxidation has led to the production of low-pH pore waters ( $pH < 0.5$ ) and the extensive dissolution of aluminosilicate minerals. Blowes (1990) noted increased concentrations of Al and Si (up to 2500 mg/L and 200 mg/L, respectively) due to the dissolution of the aluminosilicate minerals. In the deeper tailings, a diverse silicate gangue was observed, including chlorite, muscovite, quartz, and an Fe-bearing amphibole. In the upper 30 cm of the tailings, a less diverse silicate gangue, extensively depleted in chlorite and amphibole, was observed. The order of depletion of the aluminosilicate minerals followed closely the order predicted on the basis of the zero point of charge (ZPC) of the aluminosilicate mineral.

Johnson et al. (2000) documented the depletion of aluminosilicates at the Nickel Rim mine-tailings impoundment. There solid-phase Al and biotite are depleted in the upper oxidized portion of the tailings, whereas biotite is abundant in the underlying unoxidized tailings. At the Sherridon tailings impoundment, Manitoba, Moncur et al. (2003) observed extensive depletion of

biotite, chlorite, and, possibly, smectite in the upper 1 m of the tailings. At this site, there is evidence of secondary replacement of other aluminosilicates, namely, plagioclase, cordierite, and amphibole. At Sherridon, the first appearance of biotite occurs at 72 cm, which coincides with the first appearance of secondary sulfides (marcasite). Chlorite and smectite first appear at a 90 cm depth, indicating the greater tendency for dissolution. In a controlled laboratory experiment using a 0.1 M  $\text{H}_2\text{SO}_4$  solution, Jurjovec et al. (2002) observed extensive depletion of chlorite and minor depletion of biotite as a result of acid leaching of the tailings.

#### *5.4.1.4 Development of pH-buffering sequences*

The sequence of pH-buffering reactions observed within tailings impoundments results in a progressive increase in the pore-water pH along the groundwater flow path. These changes in pH occur as long zones of relatively uniform pH, which are dominated by a single-pH buffering reaction, separated by fronts or relatively sharp changes in pH as a buffering phase is depleted (Figure 3). Field data from the Nickel Rim tailings impoundment, as were presented by Johnson et al. (2000), illustrate a pH-buffering sequence. At the Nickel Rim site, the pH of the pore water at the base of the impoundment is near neutral, varying from 6.5 to 7.0. Geochemical calculations suggest that the pore water in this zone approaches or attains equilibrium with respect to calcite. Overlying the calcite-buffered zone, calcite is absent from the tailings and the pH is buffered by the dissolution of siderite and possibly by the dissolution of dolomite. The complete depletion of carbonate minerals is accompanied by a sharp decline in pH from 5.8 to 4.5. Immediately above the depth of carbonate-mineral depletion, the pH is relatively uniform, varying from 4.0 to 4.5, the dissolved Al concentrations increase sharply, and the pore water approaches or attains equilibrium with respect to gibbsite. Near the surface of the impoundment, the pH decreases

sharply from 4.0 to 3.5, then more gradually from 3.5 to approximately 2.5. Throughout this decrease in pH the pore water is undersaturated with respect to ferrihydrite, and approaches equilibrium with respect to goethite.

## 5.5 GEOCHEMISTRY AND MINERALOGY OF SECONDARY MINERALS

In mine-waste settings, the secondary minerals are those that form after disposal of the wastes. Thus, the mined material may contain both the primary, fresh minerals and the oxidation products that were formed through geological processes. In rare cases a mineral deposit will consist wholly of oxidized material, but in the acid drainage setting all of these minerals are deemed to constitute the primary assemblage because they were formed prior to disposal as wastes. After final discharge, or even during temporary storage of wastes and low-grade ores, crystallization of secondary minerals occurs *in situ* principally as a result of oxidation of the primary sulfide assemblage. However, upon removal from its disposal site, as occurs during a sampling program, a waste may form additional minerals as the material dries; such products, which are predominantly water-soluble salts that crystallize during evaporation of the pore water, are classified as 'tertiary' minerals (Jambor, 1994; Jambor and Blowes, 1998).

### 5.5.1. Soluble Sulfates: Iron Minerals

The most common secondary Fe-sulfate minerals associated with oxidized mine wastes are of the type  $\text{Fe}^{2+}\text{SO}_4 \cdot n\text{H}_2\text{O}$ , wherein  $n$  ranges from 7 to 1. The minerals of most frequent occurrence and abundance are melanterite ( $n = 7$ ), rozenite ( $n = 4$ ), and szomolnokite ( $n = 1$ ); the pentahydrate (siderotil) and hexahydrate (ferrohexahydrite) have also been reported, but are much less widespread and occur sparingly. The divalent salts seem to form in the earliest stages



of sulfide-mineral oxidation, but they are observed more commonly as superficial evanescent coatings that appear during dry periods and are susceptible to solubilization during rainfall events. Melanterite has been reported from several localities as a precipitate from greenish pools of Fe-rich solutions that drained from pyritiferous deposits, and the mineral has also been noted to form a hardpan layer in pyrite-rich tailings at the Heath Steele mine, New Brunswick, Canada (Blowes et al., 1992). The tetrahydrate, rozenite, more typically forms as a dehydration product of melanterite.

Although the soluble salts of ferric iron may crystallize on a micro scale in the earliest stages of Fe-sulfide oxidation, in field settings the paragenesis indicates that the progression is from the early formation of the divalent salts of Fe, to minerals containing both ferrous and ferric Fe, and thence to the trivalent Fe minerals (Jambor et al., 2000a,b). For minerals devoid of other cations, the most commonly occurring of the mixed-valence type is copiapite  $[\text{Fe}^{2+}\text{Fe}_4^{3+}(\text{SO}_4)_6(\text{OH})_2 \cdot 20\text{H}_2\text{O}]$ , and less common is römerite  $[\text{Fe}^{2+}\text{Fe}_2^{3+}(\text{SO}_4)_4 \cdot 14\text{H}_2\text{O}]$ . Among the trivalent-Fe minerals, the most common are coquimbite  $[\text{Fe}_2^{3+}(\text{SO}_4)_3 \cdot 9\text{H}_2\text{O}]$ , ferricopiapite  $[\text{Fe}_{2/3}^{3+}\text{Fe}_4^{3+}(\text{SO}_4)_6(\text{OH})_2 \cdot 20\text{H}_2\text{O}]$ , and rhomboclase  $[(\text{H}_3\text{O}_2)^{1+}\text{Fe}^{3+}(\text{SO}_4)_2 \cdot 2\text{H}_2\text{O}]$ . Also common is fibroferrite  $[\text{Fe}^{3+}(\text{SO}_4)(\text{OH}) \cdot 5\text{H}_2\text{O}]$ , which, however, is relatively insoluble except in acidic conditions.

A notable locality for acid drainage is Iron Mountain, California, where oxidation of pyritiferous massive sulfide deposits has resulted in the formation of many of the aforementioned soluble salts in the underground workings. The precipitation order of the salts at Iron Mountain follows the divalent to trivalent trend (Nordstrom and Alpers, 1999b).

### 5.5.2. Soluble Sulfates: Other Elements

Other than the soluble sulfates of Fe, only those of Mg and Al are of moderately common occurrence in association with acid drainage. The Mg salts are chiefly of the type  $\text{MgSO}_4 \cdot n\text{H}_2\text{O}$ , with epsomite [ $\text{MgSO}_4 \cdot 7\text{H}_2\text{O}$ ] and hexahydrate [ $\text{MgSO}_4 \cdot 6\text{H}_2\text{O}$ ] the predominant minerals. Occurrences of the pentahydrate (pentahydrate) and the tetrahydrate (starkeyite), which are known from a few localities, could be categorized as rare, and the monohydrate (kieserite), although identified as a weathering product of pyritiferous shales, has not yet been observed specifically in association with acid drainage.

Whereas the oxidation of pyrite provides the principal source for the Fe analogues of the simple Mg sulfates, the chief source of the latter is dolomite [ $\text{CaMg}(\text{CO}_3)_2$ ]. Dissolution of dolomite attenuates the acidity generated by pyrite oxidation, thereby releasing Ca and Mg to form gypsum [ $\text{CaSO}_4 \cdot 2\text{H}_2\text{O}$ ], simple Mg salts, and more complex ones such as magnesiocopiapite [ $\text{MgFe}_4^{3+}(\text{SO}_4)_6(\text{OH})_2 \cdot 20\text{H}_2\text{O}$ ]. Thus, both gypsum and the Mg sulfates may form without the development of acid drainage if dolomite is sufficiently abundant to neutralize the acidity that is generated by oxidation of the associated sulfides.

The formation of soluble salts containing Al is paragenetically later than that of the simple Mg salts because Al is sourced from aluminosilicates, the dissolution of which is typically slow and requires low-pH conditions to accelerate the process. The most common soluble sulfates of Al are members of the halotrichite-pickeringite series [ $\text{Fe}^{2+}\text{Al}_2(\text{SO}_4)_4 \cdot 22\text{H}_2\text{O}$  -  $\text{MgAl}_2(\text{SO}_4)_4 \cdot 22\text{H}_2\text{O}$ ] and of less widespread occurrence are aluminocopiapite [ $\text{Al}_{2/3}\text{Fe}_4^{3+}(\text{SO}_4)_6(\text{OH})_2 \cdot 20\text{H}_2\text{O}$ ] and alunogen [ $\text{Al}_2(\text{SO}_4)_3 \cdot 17\text{H}_2\text{O}$ ].

Various soluble salts, such as kalinite [ $\text{KAl}(\text{SO}_4)_2 \cdot 11\text{H}_2\text{O}$ ], blödite [ $\text{Na}_2\text{Mg}(\text{SO}_4)_2 \cdot 4\text{H}_2\text{O}$ ],

and bilinite  $[\text{Fe}^{2+}\text{Fe}_2^{3+}(\text{SO}_4)_4 \cdot 22\text{H}_2\text{O}]$  occur sparingly but may be locally prominent. The most common of the Cu salts is chalcantite  $[\text{CuSO}_4 \cdot 5\text{H}_2\text{O}]$ . Both goslarite  $[\text{ZnSO}_4 \cdot 7\text{H}_2\text{O}]$  and gunningite  $[\text{ZnSO}_4 \cdot \text{H}_2\text{O}]$  have been reported as secondary minerals in sphalerite-bearing wastes, but the salts occur sparingly.

### 5.5.3 Less Soluble Sulfate Minerals

Gypsum has a moderate solubility in water, whereas jarosite  $[\text{KFe}_3(\text{SO}_4)_2(\text{OH})_6]$  is relatively insoluble (Table 7). The two minerals are the most abundant and widespread of the secondary minerals associated with acid drainage. Early formation of gypsum is possible because of cation availability through the dissolution of carbonate minerals. Bassanite  $[2\text{CaSO}_4 \cdot \text{H}_2\text{O}]$  has also been identified as a secondary mineral in tailings impoundments, but the quantities are minute and are insignificant relative to those of gypsum. Jarosite is, by definition, K-dominant, but as a mine-drainage precipitate it invariably is oxonium-bearing, commonly with  $\text{K} > \text{H}_3\text{O} > \text{Na}$ . In the early stages of acid generation the bulk of the K at most localities is derived by incongruent alteration of trioctahedral mica. Various other members of the jarosite supergroup occur in acid-drainage settings; other members detected are natrojarosite  $[\text{NaFe}_3(\text{SO}_4)_2(\text{OH})_6]$ , hydronium jarosite  $[(\text{H}_3\text{O})\text{Fe}_3(\text{SO}_4)_2(\text{OH})_6]$ , plumbojarosite  $[\text{PbFe}_6(\text{SO}_4)_4(\text{OH})_{12}]$ , alunite  $[\text{KAl}_3(\text{SO}_4)_2(\text{OH})_6]$ , and As-bearing species, but all are of rare occurrence relative to jarosite.

Among the Al-sulfate salts, jurbanite  $[\text{Al}(\text{SO}_4)(\text{OH}) \cdot 5\text{H}_2\text{O}]$  is commonly used in geochemical modelling, but the mineral itself is of extremely rare occurrence; the most common Al hydroxysulfates associated with acid drainage correspond to crystalline and amorphous felsöbányaite (basaluminate)  $[\text{Al}_4(\text{SO}_4)(\text{OH})_{10} \cdot 4\text{H}_2\text{O}]$  and hydrobasaluminate  $[\text{Al}_4(\text{SO}_4)(\text{OH})_{10} \cdot 15\text{H}_2\text{O}]$ .

A poorly crystalline hydroxysulfate, schwertmannite, whose crystal structure has not yet been resolved and which is thought to have the ideal formula  $\text{Fe}_8\text{O}_8(\text{OH})_6\text{SO}_4 \cdot n\text{H}_2\text{O}$ , may be the most common direct precipitate of Fe from acidic effluents at pH 2 to 4 (Bigham and Nordstrom, 2000). The mineral is difficult to identify because of its poor crystallinity and the almost invariable presence of associated Fe oxyhydroxides and jarosite, but numerous occurrences have been reported in the recent literature. Detailed studies of the oxidation of pyrite and pyrrhotite indicate that schwertmannite is not an early-formed mineral, and the occurrences suggest an origin in which the requisite Fe and  $\text{SO}_4$  have undergone solubilization, transportation, and subsequent precipitation rather than maintaining an intimate association with precursor sulfides.

The principal ore mineral of Pb is galena  $[\text{PbS}]$ , and the predominant sulfates derived from it are anglesite  $[\text{PbSO}_4]$  and plumbojarosite. Partial substitution of Pb for the alkali-site cations also occurs in other members of the jarosite supergroup. An unusual sink for Cu and Al is the mineral hydrowoodwardite  $[\text{Cu}_{1-x}\text{Al}_x(\text{OH})_2(\text{SO}_4)_{x/2}(\text{H}_2\text{O})_n]$ , recently discovered as a supergene product at several old mines in Saxony, Germany (Witzke, 1999). The same mineral was almost simultaneously reported to occur as bluish coatings on weathered waste rocks and in stream sediments at two former mines in northern Italy (Dinelli et al., 1998).

#### *5.5.4 Metal Oxides and Hydroxides*

The oxidation of Fe sulfides invariably leads to the formation of goethite  $[\alpha\text{-FeOOH}]$  both in intimate association with the sulfides and in distal precipitates. Other oxyhydroxide minerals identified as secondary precipitates are crocite  $[\gamma\text{-FeOOH}]$  and akaganéite  $[\beta\text{-FeO}(\text{OH},\text{Cl})]$ , but occurrences are generally insignificant relative to the abundance and distribution of goethite. However, lepidocrocite has been observed to be important at some sites;

for example, Roussel et al. (2000) determined the mineral to be the principal component of suspended particulate matter in drainage from an As-rich tailings impoundment in France, and Howell and Bruce (1995) observed lepidocrocite to be a significant component of ochres that precipitated from low-pH (<5) waters at the Levant mine in Cornwall, England.

Ferrihydrite, a poorly crystalline mineral of widespread occurrence, is equivalent to the compound that is commonly referred to as 'amorphous  $\text{Fe}(\text{OH})_3$ '. Precipitation of ferrihydrite is favored when oxidation of  $\text{Fe}^{2+}$  and hydrolysis occur rapidly. The mineral is unstable with respect to goethite, and precipitation occurs at a higher pH than that for schwertmannite. The presence of ferrihydrite in precipitates from mine-waste effluents is commonly reported, but unequivocal identifications of its presence in mine-waste solids, such as tailings, have been fewer. For the latter, because the crystallinity is poor and the mineral forms only a small proportion of the total waste solids, recourse is generally made to selective dissolution whereby the fraction that is more soluble in certain reagents is inferred to represent ferrihydrite rather than goethite, which is more dissolution-resistant.

Although hematite [ $\alpha\text{-Fe}_2\text{O}_3$ ] is a common product of the oxidation of sulfide-bearing mineral deposits, only a few unequivocal occurrences are known in mine-drainage settings (e.g., Hochella et al., 1999; Boulet and Larocque, 1996). Various Fe oxides and oxyhydroxides, including hematite, maghemite [ $\gamma\text{-Fe}_2\text{O}_3$ ], and ilmenite [ $\text{Fe}^{2+}\text{TiO}_3$ ] have been observed as microcrystalline aggregates that have formed within acidophilic microorganisms in sediments affected by effluents from tailings at Elliot Lake, Ontario, Canada (Mann and Fyfe, 1989). Minerals of the spinel group, which includes magnetite [ $\text{Fe}^{2+}\text{Fe}_2^{3+}\text{O}_4$ ], have been detected, but most associations are on a minute scale. However, the presence of extensive accumulations of magnetite derived by the anoxic reduction of transported Fe in mining-impacted lake-bottom

sediments has been reported by Cummings et al. (2000).

Manganese oxides-oxyhydroxides have been observed at a few acid-drainage localities. For example, Benvenuti et al. (2000) observed pyrolusite  $[\text{MnO}_2]$  and pyrochroite  $[\text{Mn}(\text{OH})_2]$  in weathered jig tailings and waste rock at a site in Tuscany, Italy. Hochella et al. (1999) identified hydrohetaerolite  $[\text{Zn}_2\text{Mn}_4^{3+}\text{O}_8\cdot\text{H}_2\text{O}]$  among the secondary minerals in stream sediments at an acid drainage site in Montana, and nsutite  $[\gamma\text{-MnO}_2]$ , birnessite  $[\text{Na}_4\text{Mn}_{14}\text{O}_{27}\cdot 9\text{H}_2\text{O}]$ , and minerals in the ranciéite-takanelite series  $[(\text{Ca},\text{Mn}^{2+})\text{Mn}_4^{4+}\text{O}_9\cdot 3\text{H}_2\text{O} - (\text{Mn}^{2+},\text{Ca})\text{Mn}_4^{4+}\text{O}_9\cdot\text{H}_2\text{O}]$  were among the various Mn minerals detected in precipitates in the streambed of Pinal Creek, Arizona (Lind and Hem, 1993). At Pinal Creek, the acidic groundwater plume reacted with calcite-bearing alluvium, initially forming 'amorphous Fe oxide' as pH increased, and subsequently precipitating the Mn-bearing assemblage farther downstream, where the pH of the stream water was near neutral. Similar relationships were observed by Hudson-Edwards et al. (1996), who identified cesarolite  $[\text{PbH}_2\text{Mn}_3\text{O}_8]$ , coronadite  $[\text{Pb}(\text{Mn}^{4+},\text{Mn}^{2+})_8\text{O}_{16}]$ , woodruffite  $[(\text{Zn},\text{Mn}^{2+}\text{Mn}_3^{4+}\text{O}_7\cdot 1\text{-}2\text{H}_2\text{O})]$ , and hydrohetaerolite in contaminated stream sediments of the Tyne River catchment, northeastern England, and noted the disappearance of these minerals in downstream areas in which the pH of the water was lower.

The presence of plumboferrite  $[\sim\text{PbFe}_4\text{O}_7]$  in the Tyne River sediments was reported by Hudson-Edwards et al. (1996), and the mineral has also been identified as a secondary product in tailings (Morin et al., 1999). Although Al hydroxides play a prominent role in geochemical modelling, few occurrences of such material have been described. Bove et al. (2000) reported the presence of an X-ray amorphous Al hydroxide precipitate in a stream channel that drains an acid-sulfate hydrothermal system near Silverton, Colorado, and Berger et al. (2000) reported the

occurrence of a poorly crystalline Al hydroxide in particulate matter that was filtered from seeps below an abandoned waste-rock dump in New Mexico; however, detailed characterizations were not published. Diaspore [AlOOH] has been reported to occur as a secondary mineral in a waste-rock dump in Tuscany, Italy (Benvenuti et al., 1997). In the study by Hochella et al. (1999), a nearly pure amorphous Si-Al oxyhydroxide (Si:Al = 2:1) rather than Al(OH)<sub>3</sub> was identified as the major sink for Al in the local drainage system.

The occurrence of secondary SiO<sub>2</sub>·*n*H<sub>2</sub>O has been observed in several tailings impoundments, predominantly as amorphous hydrated pseudomorphs after biotite. Cristobalite [SiO<sub>2</sub>] has also been detected in the pseudomorphs. Partial replacement of various other minerals by amorphous silica has also been observed.

An extensive suite of supergene minerals, including chlorides, sulfates, and arsenates occurs at the Levant mine, Cornwall, England, where ingress of sea water has influenced the variety of minerals in the suite. In stagnant pools of mine drainage at the mine, cuprite [Cu<sub>2</sub>O] and native copper have precipitated within the ochres (Bowell and Bruce, 1995).

#### *5.5.5 Carbonate Minerals*

Like the precipitation of secondary Al(OH)<sub>3</sub>, that of secondary siderite [FeCO<sub>3</sub>] is widely employed in geochemical models. Secondary siderite and associated Fe oxyhydroxides were determined to have formed as coatings, up to 1000 nm thick, on ankerite-dolomite in the Kidd Creek tailings impoundment at Timmins, Ontario, Canada (Al et al., 2000). At Elliot Lake, Ontario, nodules of siderite, each <10 µm across, and calcite in aggregates up to 400 µm across, occur as secondary minerals in a small tailings impoundment (Paktunc and Davé, 2002). The precipitation of the carbonate minerals at the Elliot Lake site was interpreted to result from high

alkalinity related to the presence of decaying organic debris.

At the Matchless pyritiferous deposit in Namibia, huntite  $[\text{CaMg}_3(\text{CO}_3)_4]$  occurs within high-pH zones in an oxidized tailings impoundment (Dill et al., 2002). The high-pH zones are sandwiched between low-pH layers, with phyllosilicate-rich layers acting as aquitards that impede vertical movement and homogenization of the pore waters.

Wastes from Pb-rich mineral deposits typically form anglesite in sulfate-dominant environments, but in limestone-dominated host rocks and in gangue containing abundant carbonates, both cerussite  $[\text{PbCO}_3]$  and hydrocerussite  $[\text{Pb}_3(\text{CO}_3)_2(\text{OH})_2]$  have been reported as secondary minerals in mining-related wastes. Several carbonate and hydroxycarbonate minerals of Cu and Zn were reported by Hudson-Edwards et al. (1996) as secondary products in stream sediments in the Tyne Basin, England.

#### 5.5.6 Arsenates and Phosphates

Secondary phosphates occur rarely in acid-drainage settings. Pyromorphite  $[\text{Pb}_5(\text{PO}_4)_3\text{Cl}]$  has been identified in tailings (Morin et al., 1999) and in mining-related stream sediments (Hudson-Edwards et al., 1996). Brushite  $[\text{CaHPO}_4 \cdot 2\text{H}_2\text{O}]$  was reported by Dill et al. (2002) to be present in the oxidized tailings of the Matchless mine, Namibia, but the absence of an adequate source of  $\text{PO}_4$  in the primary mineral assemblage indicated that the anion was most likely derived from a flotation reagent.

Arsenates are much more common than phosphates in mine-drainage settings, mainly because of the presence of arsenopyrite  $[\text{FeAsS}]$  and arsenical pyrite as primary sources of As in metalliferous deposits. For many years the processing of arsenical gold ores involved roasting of the sulfide concentrates, and the off-gases and particulate emissions were dispersed to the



atmosphere and surrounding countryside. Subsequent technological improvements led to recovery of the As-rich emissions, principally by condensation as  $\text{As}_2\text{O}_3$  (arsenolite), the disposal of which has in turn created environmental problems. For example, more than 100,000 tonnes of  $\text{As}_2\text{O}_3$  are temporarily stored in the underground workings of the gold mines at Yellowknife, Canada, and permanent disposal is a major environmental concern. At a site near Marseille, France, wastes from the processing of arsenical ores contain pyrite, arsenopyrite, and arsenolite, and runoff waters are As-rich and low in pH (2.2). The flows subsequently interact with a limestone substratum, thereby raising the pH and precipitating white crusts that contain gypsum, pharmacolite  $[\text{CaHAsO}_4 \cdot 2\text{H}_2\text{O}]$ , haidingerite  $[\text{CaHAsO}_4 \cdot \text{H}_2\text{O}]$ , weilite  $[\text{CaHAsO}_4]$ , and micropharmacolite  $[\text{H}_2\text{Ca}_4\text{Mg}(\text{AsO}_4)_4 \cdot 11\text{H}_2\text{O}]$ ; scorodite  $[\text{FeAsO}_4 \cdot 2\text{H}_2\text{O}]$  was also identified in the filtered particulate matter (Juillot et al., 1999).

Scorodite and pharmacosiderite  $[\text{KFe}^{3+}(\text{AsO}_4)_3(\text{OH})_4 \cdot 6-7\text{H}_2\text{O}]$  have been observed in the wastes at abandoned mines (e.g., Brown et al., 1990). At the Mole River mine, Australia, which ceased the processing of arsenopyrite ore in the 1930s and is known as a source of acid drainage and As contamination, Ashley and Lottermoser (1999) identified scorodite in the regionally contaminated soils. The stream sediments contain arsenolite, and at the mine and roaster is a mixed assemblage that includes pharmacolite and clinoclase  $[\text{Cu}_3(\text{AsO}_4)(\text{OH})_3]$ . Gypsum, pharmacolite, and krautite  $[\text{MnH}(\text{AsO}_4) \cdot \text{H}_2\text{O}]$  occur as efflorescences at the furnace.

Acidic drainage (pH 2.2-4) from a former Pb-Zn mine in Gard, France, was determined by Leblanc et al. (1996) to average  $250 \text{ mg L}^{-1}$  As, and ochreous downstream sediments contain up to 20 wt% As in stromatolite-like accreted material up to 20 cm thick. Precipitation of the accreted material was attributed to direct or indirect microbial action. X-ray study of the material showed it to contain scorodite, poorly crystalline hematite, bukovskýite



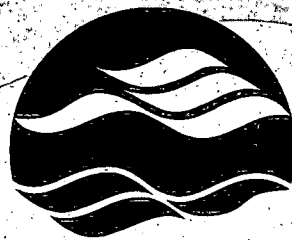
3 9055 1018 1981 0

PRINTED IN CANADA  
IMPRIMÉ AU CANADA



ON RECYCLED PAPER  
SUR DU PAPIER RECYCLÉ

**National Water Research Institute**  
**Environment Canada**  
**Canada Centre for Inland Waters**  
P.O. Box 5050  
867 Lakeshore Road  
Burlington, Ontario  
L7R 4A6 Canada



**NATIONAL WATER  
RESEARCH INSTITUTE**  
**INSTITUT NATIONAL DE  
RECHERCHE SUR LES EAUX**

**National Hydrology Research Centre**  
11 Innovation Boulevard  
Saskatoon, Saskatchewan  
S7N 3H5 Canada

**Institut national de recherche sur les eaux**  
**Environnement Canada**  
**Centre canadien des eaux intérieures**  
Case postale 5050  
867, chemin Lakeshore  
Burlington, Ontario  
L7R 4A6 Canada

**Centre national de recherche en hydrologie**  
11, boul. Innovation  
Saskatoon, Saskatchewan  
S7N 3H5 Canada



Environment  
Canada

Environnement  
Canada

**Canada**